

# A DNA-based molecular probe for optically reporting cellular traction forces

Brandon L Blakely<sup>1,10</sup>, Christoph E Dumelin<sup>2,10</sup>, Britta Trappmann<sup>3,4,10</sup>, Lynn M McGregor<sup>5,6</sup>, Colin K Choi<sup>3,4</sup>, Peter C Anthony<sup>7</sup>, Van K Duesterberg<sup>7</sup>, Brendon M Baker<sup>3,4</sup>, Steven M Block<sup>8,9</sup>, David R Liu<sup>5,6</sup> & Christopher S Chen<sup>1,3,4</sup>

**We developed molecular tension probes (TPs) that report traction forces of adherent cells with high spatial resolution, can in principle be linked to virtually any surface, and obviate monitoring deformations of elastic substrates. TPs consist of DNA hairpins conjugated to fluorophore-quencher pairs that unfold and fluoresce when subjected to specific forces. We applied TPs to reveal that cellular traction forces are heterogeneous within focal adhesions and localized at their distal edges.**

Traction forces are critical for many cellular processes, including migration, proliferation and differentiation<sup>1–4</sup>. Despite the central role played by such forces in cell function, the primary technique to measure them uses elastic substrates including polyacrylamide gels or elastomeric posts<sup>5,6</sup>. The elasticity of these materials itself modulates cellular tractions, adhesion and function<sup>7–9</sup>, thereby confounding the measurement. Furthermore, the spatial resolution of conventional methods to measure traction forces is typically limited to micrometers by the sizes of substrate deformations or by the density of posts or other fiducial markers used to map the deformations<sup>10</sup>. To overcome this limit, Salaita and coworkers recently described a molecular force sensor in which an entropic poly(ethylene glycol) (PEG) spring separates a fluorescence resonance energy transfer pair<sup>11</sup>. Although this technique is promising, it is difficult to tune the stiffness of this spring to capture different ranges of relevant forces. Wang and Ha reported an alternative approach using dsDNA, wherein the sequence and length of base-pair complementarity can tune the force required to pull apart the strands<sup>12</sup>. In this system, the detachment of cells provides a quantitative measure of forces, but no spatiotemporal resolution.

To address these limitations, we engineered a new class of molecular TPs that spatiotemporally report traction forces on the basis of DNA hairpins. DNA hairpins unfold in response to precise amounts of force<sup>13,14</sup> that can be tuned by varying the length and composition of the DNA sequence<sup>15,16</sup>. We conjugated DNA hairpins of various stem lengths and sequences to different fluorophore-quencher pairs such that fluorophores were quenched in the folded state but fluoresced in the unfolded state (Supplementary Fig. 1 and Supplementary Tables 1–3). The 5' end of each hairpin was conjugated to the GGRGDS peptide, which binds integrin adhesion receptors<sup>17</sup>. Although we chose the well-established RGD sequence to provide cell-adhesive functionality for this study, the synthesis could be modified to attach different peptides, or larger proteins, through either their N termini or lysine side chains. The 3' end of the hairpin was functionalized with a free thiol linker, enabling chemical conjugation to cell culture substrates. When a cell is attached to a substrate through TPs, TP fluorescence enables the reversible, optical measurement of cell traction forces (Fig. 1a).

We used a dual-beam optical trapping apparatus to determine the forces needed to open TP constructs. We tested whether the chemical modifications made to these nucleic acids (including the attachment of a fluorophore-quencher pair and the addition of the PEG spacer) or the composition of the cell culture medium used for live-cell experiments perturbed the values previously determined for DNA hairpins with otherwise similar sequences<sup>16</sup> (Fig. 1b). Single TPs were attached to DNA handles and held in a 'dumbbell' arrangement between two optically trapped beads; we then subjected the TPs to a range of loads, using a force clamp to determine the  $F_{1/2}$  value at room temperature, the force at which the hairpin spends equal time in its folded and unfolded states. The  $F_{1/2}$  values for chemically modified hairpins in culture medium did not differ substantially from values obtained with unmodified DNA hairpins in a simple monovalent salt buffer<sup>16,18</sup> (Fig. 1c and Supplementary Table 4), suggesting that the chemical modifications and culture medium compositions did not strongly influence the forces needed to open various TP hairpins. Because cell cultures are maintained at 37 °C, correction factors were applied to the measured  $F_{1/2}$  values to estimate opening forces at 37 °C:  $F_{1/2}^*$  (Supplementary Table 1).

We plated mouse embryonic fibroblasts (MEFs) on TP-conjugated glass substrates and imaged cell-generated force signals via total-internal-reflection fluorescence (TIRF) microscopy. Strong fluorescence signals over background noise (500:1) were detected that mirrored the sizes, shapes and locations of focal adhesions

<sup>1</sup>Department of Bioengineering, University of Pennsylvania, Philadelphia, Pennsylvania, USA. <sup>2</sup>X-Chem, Inc., Waltham, Massachusetts, USA. <sup>3</sup>Department of Biomedical Engineering, Boston University, Boston, Massachusetts, USA. <sup>4</sup>The Wyss Institute for Biologically Inspired Engineering, Harvard University, Boston, Massachusetts, USA. <sup>5</sup>Department of Chemistry and Chemical Biology, Harvard University, Cambridge, Massachusetts, USA. <sup>6</sup>Howard Hughes Medical Institute, Harvard University, Cambridge, Massachusetts, USA. <sup>7</sup>Biophysics Program, Stanford University, Stanford, California, USA. <sup>8</sup>Department of Biology, Stanford University, Stanford, California, USA. <sup>9</sup>Department of Applied Physics, Stanford University, Stanford, California, USA. <sup>10</sup>These authors contributed equally to this work. Correspondence should be addressed to C.S.C. (chencs@bu.edu).

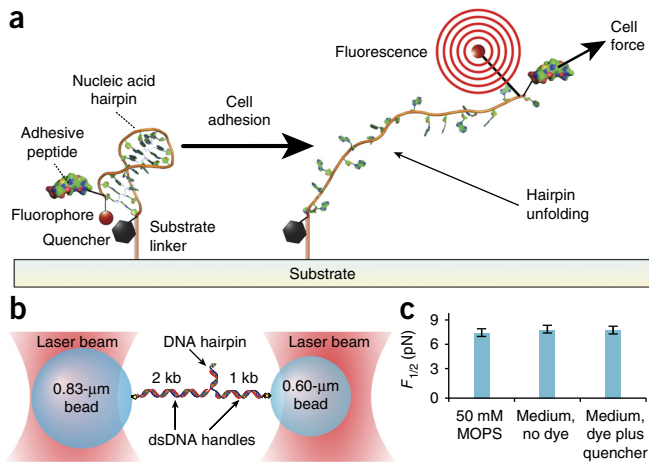


**Figure 1** | Design and characterization of DNA hairpin force probe.

(a) Schematic depiction of the TPs. A DNA hairpin is functionalized with a fluorophore-quencher pair, covalently conjugated by the 3' end of the hairpin to a solid substrate and conjugated at its 5' end, via a PEG spacer, to the integrin-binding peptide RGD. Upon the application of sufficient force to unfold the hairpin, the fluorophore separates from the quencher and fluoresces. (b) Schematic of the experimental geometry used to characterize the mechanics of the hairpins. The DNA hairpin is attached at each end to dsDNA handles bound to optically trapped beads (not to scale) in a force-clamped arrangement. (c) Measured  $F_{1/2}$  (hairpin opening force) values as a function of medium and fluorophore-quencher conjugation at 21 °C (mean  $\pm$  s.e.m.).  $n \geq 3$  for each condition.

(FAs) (Fig. 2a, Supplementary Figs. 2–5 and Supplementary Table 5). Time-lapse imaging revealed that TP fluorescence appeared, shifted, disappeared and reappeared dynamically, reminiscent of adhesion assembly-disassembly dynamics (Supplementary Video 1). TPs with different fluorophores (fluorescein, Alexa 546 and Alexa 647) and different  $F_{1/2}$  values, ranging from 5.7 to 16.5 pN, all exhibited similar responses to attached cells (Supplementary Figs. 5–7). When we cultured cells on a surface coated with an equimolar mixture of two TPs with different  $F_{1/2}$  values, both TPs reported the same magnitude and pattern of traction stresses in cells. The ratio of signal intensity between the two TPs was constant across the range of observed cellular forces, suggesting that TP fluorescence signal and traction force have a simple linear relationship across this range (Supplementary Fig. 6).

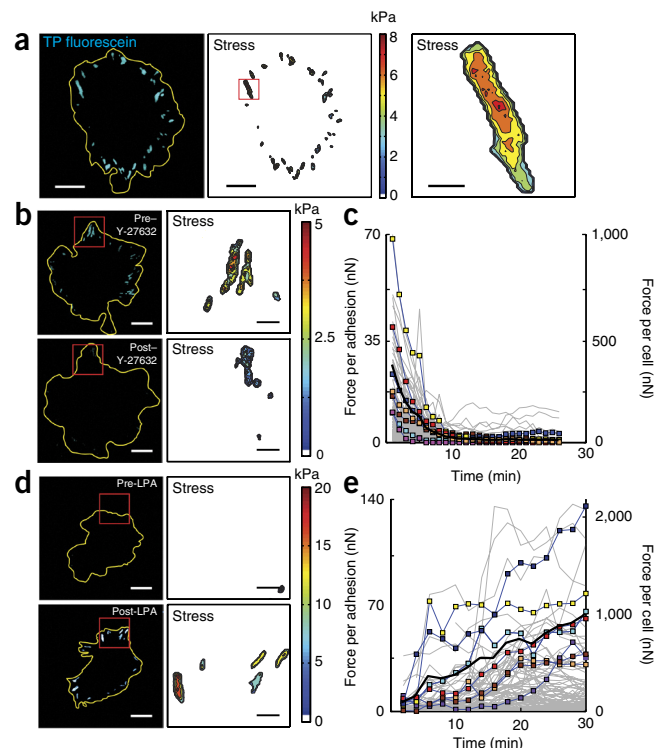
The fluorescence signal reports the number of unfolded TPs per pixel and therefore may be used to infer the lower bound of traction stress (force per unit area) applied at the surface (Online Methods). The resulting stress maps revealed mean traction levels per adhesion ( $\sim 1$  kPa) that are consistent with previous estimates calculated by assuming that forces were evenly distributed across the area of adhesions<sup>19</sup>. These maps, however, revealed that the spatial distribution of traction stresses between, and within, each FA is strikingly heterogeneous, with stresses peaking as high as 30 kPa (Fig. 2a). To confirm that the fluorescence signals reflected traction forces, we examined the effects of either suppressing or enhancing cell contractility. Addition of Y-27632, an inhibitor of contraction<sup>20</sup>, rapidly extinguished traction signals distributed in large adhesions

to dim, punctate signals (Fig. 2b,c and Supplementary Video 2). Conversely, treatment of starved cells with lysophosphatidic acid (LPA), a strong stimulant of contraction<sup>21</sup>, led to a rapid growth of bright foci again reminiscent of FAs (Fig. 2d,e and Supplementary Video 3). Together, these results suggest that the observed fluorescence signals reflect bona fide changes in cellular traction forces.

Diminished surface density of adhesive ligand lowers the total force that cells exert<sup>22</sup>, but the forces experienced by individual adhesions are unknown. Consistent with prior studies, decreasing stoichiometries of the TP and its non-adhesive analog lacking the RGD sequence and fluorophore resulted in less cell spreading, fewer and smaller adhesions, and lower total cell force (Supplementary Figs. 8 and 9a–f). Surprisingly, the tension per adhesion and tension per TP peaked at intermediate TP density (Supplementary Fig. 9g,h), implying that adhesive ligand-induced activation of cellular contractility occurs at a lower ligand density than that of ligand-induced adhesion assembly.

TPs offer a substantial improvement in spatial resolution compared to traditional traction force methods, which typically report forces on a scale of several micrometers<sup>23</sup>. Because TPs are single fluorescent molecules, the resolution of traction force

**Figure 2** | Fluorescence reports cellular traction forces. (a) MEF attached on a TP-coated substrate. Fluorescence signals from TPs beneath a spread cell (yellow outline) were acquired (left) and then converted to traction stress maps calculated from the fluorescence level (center). The traction stress map of an individual adhesion site is shown (right). Scale bars, 20  $\mu\text{m}$  (left and center) and 3  $\mu\text{m}$  (right). (b,d) Fluorescence (left) and traction map (right) reported by TPs of cells spread before (top) and after (bottom) addition of either the ROCK inhibitor Y-27632 (15 min after treatment) (b) or lysophosphatidic acid (LPA) (1 h after treatment), an activator of Rho (d). Scale bars, 20  $\mu\text{m}$  (left) and 5  $\mu\text{m}$  (right). (c,e) Mean stress per adhesion site as a function of time for individual cells treated with Y-27632 (c) or LPA (e). Gray lines, individual adhesions; colored squares and lines, individual cells; black solid line, mean of all cells.  $n \geq 7$  cells and 650 adhesions. TP calibrations were carried out using the  $F_{1/2}$  values for 37 °C (Supplementary Table 1).



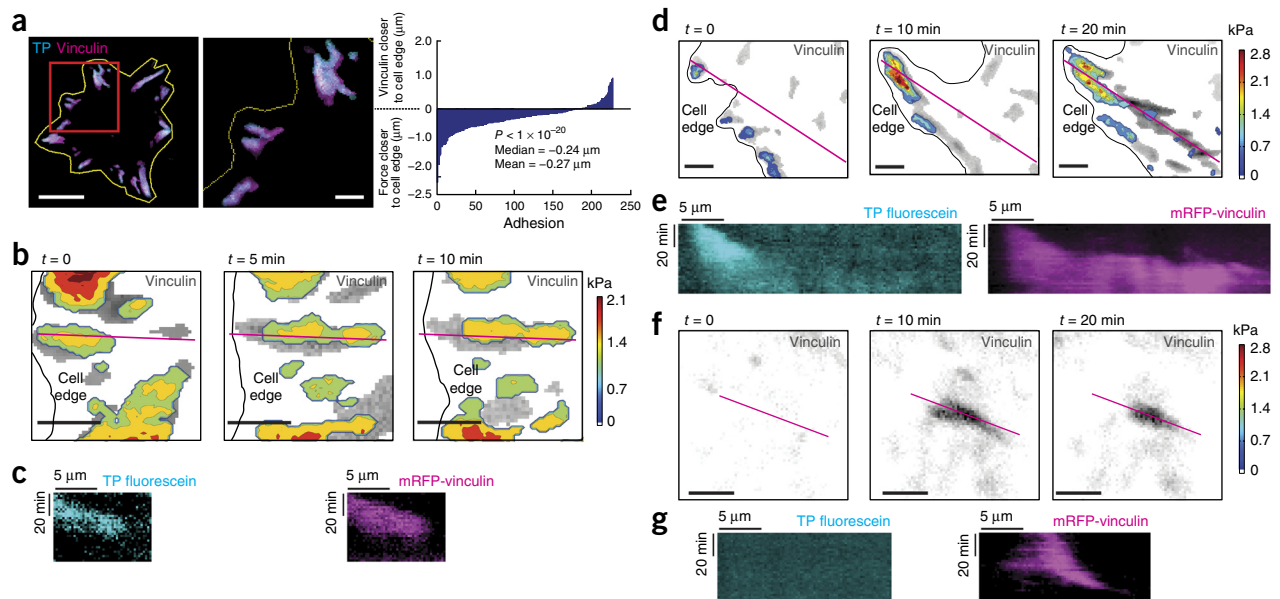


**Figure 3** | Localization of traction forces with respect to FA proteins. (a) Fluorescence image of TP-coated substrate (cyan) and overlying cell (yellow outline) expressing mRFP-vinculin (magenta). A high-magnification inset is shown (center). The plot shows the difference in distance (in  $\mu\text{m}$ ) of the geometric centroid from the cell edge of the two signals for selected adhesions (right). The skew in the distribution reflects a distal bias for tractions relative to adhesions. ( $P$  value reported from Wilcoxon signed-rank test of difference between distances of centroids of adhesions from the cell edge as reported by TPs and mRFP-vinculin.) Scale bars, 20  $\mu\text{m}$  (left) and 5  $\mu\text{m}$  (center).  $n = 7$  cells and 227 adhesions. (b–g) Representative examples of the three classes of adhesions. Images show a sequence over time of the vinculin fluorescence (grayscale) overlaid with the TP-reported stress map (b,d,f). Scale bars, 5  $\mu\text{m}$ . Black outline, cell edge; magenta line, position used for kymographs (c,e,g) showing the evolution of the TP (left) and vinculin (right) signals over time. TP calibrations were carried out using the  $F_{1/2}$  values for 37  $^{\circ}\text{C}$  (Supplementary Table 1). 112 adhesions were cataloged using this analysis: 86 where force and assembly-disassembly were correlated, 12 where force localized only to the tip of a growing adhesion, and 14 that spontaneously formed without force.

measurements is dictated by photon capture efficiency and microscope optics (in this work, 200 nm  $\times$  200 nm image pixels). To demonstrate the utility of this resolution, we cultured MEFs expressing mRFP-tagged vinculin, a scaffolding protein that localizes to FAs, and compared the distribution of vinculin to the distribution of TP signal. The locations and geometries of traction foci correlated strongly with those of FAs; however, the TP foci were consistently closer to the cell edge than vinculin foci by  $\sim 200$  nm (Fig. 3a and Supplementary Fig. 5). Two recent studies using traction force microscopy on elastic gels also reported forces focused to distal edges<sup>24,25</sup>, but it is difficult to interpret whether the larger spatial shift (1.4  $\mu\text{m}$ ) reported in those studies is due to differences in resolution or substrate stiffness.

Following the evolution of traction forces and FAs, we also observed three distinct classes of adhesions. In one class, traction force and vinculin location correlated to a high degree throughout the lifetime of the adhesion; force increased during adhesion assembly and subsided during its disassembly (86 of the 112 adhesions cataloged; Fig. 3b,c). In a second class, force and vinculin colocalized at the initiation of the adhesion, but as the adhesion continued to grow and extend toward the center of the cell, force remained localized to the distal tip of the elongating adhesion (12 of 112 adhesions; Fig. 3d,e). In a third class of adhesions, which formed in the cell interior well behind lamellipodia, no force was observed despite vinculin clustering (14 of 112 adhesions; Fig. 3f,g). Time-lapse studies highlighted the heterogeneity of stress experienced within any given adhesion: some exhibited a single concentrated peak of stress; some showed multiple peaks that appeared, disappeared, merged or split; and some showed a plateau in stress,

with no concentrated peaks. All together, these findings reveal a complex orchestration of cellular forces within FAs.

This study establishes DNA hairpins as versatile molecular reporters to study cellular forces. Methods to measure traction forces using elastic substrates have been instrumental in establishing the importance of forces<sup>26</sup>. Although molecular TPs are currently unable to provide directional information about forces, their improved resolution, their ability to attach to arbitrary substrates and the versatility that should be possible by coupling different adhesive ligands all afford special advantages in elucidating the contribution of cellular forces to cell adhesion and function. Previous studies have coupled elastic chains and fluorescence resonance energy transfer probes to report forces across vinculin and epidermal growth factor receptor<sup>27,28</sup>. The TPs developed here, by contrast, generate a higher signal-to-noise ratio owing to the substantial change in fluorescence as a function of fluorophore-quencher distance. Furthermore, the well-established relationship between DNA sequence and DNA folding energetics<sup>16</sup> enables the rational design of TPs for sensing force over various ranges of interest. Although the investigation of DNA mechanics has largely been used to establish fundamental models of polymer physics, using these physical principles to engineer DNA-based probes that report molecular forces may enable a new class of measurement tools and provide new insights into forces generated by living systems at the cellular level.

## METHODS

Methods and any associated references are available in the [online version of the paper](#).

Note: Any Supplementary Information and Source Data files are available in the online version of the paper.

#### ACKNOWLEDGMENTS

This work was supported in part from grants from the US National Institutes of Health (EB00262, EB08396, EB001046, HL115553, GM065865, GM74048 and GM57035) and Howard Hughes Medical Institute. We thank M. Woodside for assistance in modeling hairpin opening forces. We thank R. Assoian (University of Pennsylvania) for providing MEFs. B.L.B., C.K.C., B.M.B. and C.E.D. acknowledge fellowships from the US National Science Foundation, American Heart Association, Ruth L. Kirschstein National Research Service Award and Novartis Foundation, respectively.

#### AUTHOR CONTRIBUTIONS

B.L.B., C.E.D., C.S.C. and D.R.L. conceived of and initiated the project. B.L.B., C.E.D., B.T., L.M.M., C.K.C., P.C.A., V.K.D. and B.M.B. designed, performed, analyzed and interpreted experiments. C.E.D., B.T. and L.M.M. synthesized TPs. P.C.A. and V.K.D. characterized TP mechanics. B.L.B., B.T., C.K.C. and B.M.B. performed the cell-based experiments. S.M.B., C.S.C. and D.R.L. supervised the project.

#### COMPETING FINANCIAL INTERESTS

The authors declare no competing financial interests.

Reprints and permissions information is available online at <http://www.nature.com/reprints/index.html>.

1. Beningo, K.A. & Wang, Y.L. *Trends Cell Biol.* **12**, 79–84 (2002).
2. Mammoto, T. & Ingber, D.E. *Development* **137**, 1407–1420 (2010).
3. McBeath, R., Pirone, D.M., Nelson, C.M., Bhadriraju, K. & Chen, C.S. *Dev. Cell* **6**, 483–495 (2004).
4. Pirone, D.M. *et al. J. Cell Biol.* **174**, 277–288 (2006).
5. Dembo, M. & Wang, Y.L. *Biophys. J.* **76**, 2307–2316 (1999).
6. Tan, J.L. *et al. Proc. Natl. Acad. Sci. USA* **100**, 1484–1489 (2003).
7. Engler, A.J., Sen, S., Sweeney, H.L. & Discher, D.E. *Cell* **126**, 677–689 (2006).
8. Paszek, M.J. *et al. Cancer Cell* **8**, 241–254 (2005).
9. Pelham, R.J. Jr. & Wang, Y. *Proc. Natl. Acad. Sci. USA* **94**, 13661–13665 (1997).
10. Legant, W.R. *et al. Nat. Methods* **7**, 969–971 (2010).
11. Liu, Y., Yehl, K., Narui, Y. & Salaita, K. *J. Am. Chem. Soc.* **135**, 5320–5323 (2013).
12. Wang, X. & Ha, T. *Science* **340**, 991–994 (2013).
13. Kong, F., Garcia, A.J., Mould, A.P., Humphries, M.J. & Zhu, C. *J. Cell Biol.* **185**, 1275–1284 (2009).
14. Sun, Z. *et al. Am. J. Physiol. Heart Circ. Physiol.* **289**, H2526–H2535 (2005).
15. Woodside, M.T. *et al. Science* **314**, 1001–1004 (2006).
16. Woodside, M.T. *et al. Proc. Natl. Acad. Sci. USA* **103**, 6190–6195 (2006).
17. Ruoslahti, E. & Pierschbacher, M.D. *Cell* **44**, 517–518 (1986).
18. Anthony, P.C. *et al. J. Am. Chem. Soc.* **134**, 4607–4614 (2012).
19. Balaban, N.Q. *et al. Nat. Cell Biol.* **3**, 466–472 (2001).
20. Uehata, M. *et al. Nature* **389**, 990–994 (1997).
21. Yoshioka, K., Matsumura, F., Akedo, H. & Itoh, K. *J. Biol. Chem.* **273**, 5146–5154 (1998).
22. Reinhart-King, C.A., Dembo, M. & Hammer, D.A. *Langmuir* **19**, 1573–1579 (2003).
23. Sabass, B., Gardel, M.L., Waterman, C.M. & Schwarz, U.S. *Biophys. J.* **94**, 207–220 (2008).
24. Plotnikov, S.V., Pasapera, A.M., Sabass, B. & Waterman, C.M. *Cell* **151**, 1513–1527 (2012).
25. Legant, W.R. *et al. Proc. Natl. Acad. Sci. USA* **110**, 881–886 (2013).
26. Style, R.W. *et al. Soft Matter* **10**, 4047–4055 (2014).
27. Grashoff, C. *et al. Nature* **466**, 263–266 (2010).
28. Stabley, D.R., Jurchenko, C., Marshall, S.S. & Salaita, K.S. *Nat. Methods* **9**, 64–67 (2012).

## ONLINE METHODS

**Synthesis of GGRGDS.** The GGRGDS peptide was synthesized on a Tribute instrument (Protein Technologies) on a 300  $\mu\text{M}$  scale using standard Fmoc peptide synthesis protocols, Fmoc-L-Ser(tBu)-Wang resin (Chem-Impex) and 1.5 mmol amino acid/HBTU cartridges (Protein Technologies). After cleavage from the solid support and removal of protective groups from the side chains using trifluoroacetic acid/phenol/water/tri-isopropylsilane (88/5/5/2), the peptide was precipitated with ether and purified by high-pressure liquid chromatography (HPLC, Agilent Technologies 1100 series) on a Kromasil 100-5-C18 column (21.2 mm  $\times$  250 mm) by running a 0.1% trifluoroacetic acid solution for 5 min and subsequently increasing the organic phase to 20% acetonitrile over 30 min.

**Synthesis of force probes for cellular experiments.** For each force probe, two DNA fragments (A and B) were synthesized on 1  $\mu\text{mol}$  scale on a PerSeptive Biosystems Expedite 8909 DNA synthesizer, using commercially available standard base monomers and sequence modifiers. The larger fragment A contained a 5' protected thiol modifier (thiol-modifier C6 S-S, Glen Research) followed by an amino modifier (Fmoc amino-modifier C6 dT, Glen Research) and either nucleotides 1–34 of the hairpin sequence for TP9 and TP17 or nucleotides 1–19 for TP6. Alternatively, fluorescently labeled fragments were synthesized using a fluorophore-containing phosphoramidite (6-fluorescein serinol phosphoramidite, Cy3 Phosphoramidite, TAMRA-dT, Glen Research). The smaller fragment B contained the remaining nucleotides of the force probe at the 5' end, followed by a quencher (Epoch Eclipse quencher phosphoramidite, Glen Research; BBQ-650-dT CEP, Berry & Associates; BHQ-1-dT), a PEG spacer (spacer phosphoramidite 18, Glen Research) and a 3' protected thiol modifier (3' thiol modifier C6 SS CPG, Biosearch Technologies). Fragments under 20 nucleotides in length were synthesized with cleavage of the final trityl group on resin. Following solid-phase synthesis, final cleavage from the solid support and the removal of protecting groups were carried out by treatment with aqueous ammonium hydroxide and methylamine (1:1) at 65  $^{\circ}\text{C}$  for 20 min. For TAMRA-containing DNA sequences, an UltraMILD deprotection scheme was deployed following the manufacturer's instructions. The oligonucleotides were purified by reverse-phase HPLC (Agilent Technologies 1200 series), using a linear gradient from 100 mM triethyl ammonium acetate to 100% acetonitrile at 45  $^{\circ}\text{C}$  on an Eclipse XBD C18 column (5  $\mu\text{m}$ , 9.4 mm  $\times$  250 mm, Agilent) and lyophilized. If appropriate, the trityl group was removed by the addition of 3% trifluoroacetic acid followed by precipitation with 10% (v/v) 3 M NaOAc, pH 5, and 300% (v/v) ethanol.

Where appropriate, A fragments were labeled with fluorophore by incubating 100 nmol oligonucleotide and 1  $\mu\text{mol}$  fluorophore (5-carboxyfluorescein *N*-succinimidyl ester, Sigma; Alexa Fluor 546 succinimidyl ester, Life Technologies; Alexa Fluor 647 succinimidyl ester, Life Technologies) for 18 h at 25  $^{\circ}\text{C}$  in 200 mM aq.  $\text{NaHCO}_3$ , pH 8.3. Excess fluorophore was removed by ethanol precipitation of the oligonucleotide-fluorophore conjugate. The peptide was appended to the 5' thiol modification as follows: 100 mM dithiothreitol (DTT) was added to the oligonucleotide in 50 mM  $\text{Na}_2\text{HPO}_4$ , pH 8, at 25  $^{\circ}\text{C}$  for 30 min to cleave the 5' S-S bond. The reaction was purified by size-exclusion chromatography

using a NAP-5 column (GE Healthcare Life Sciences) and ethanol precipitation. 100 nmol of the thiol-containing oligonucleotide was stirred with 2  $\mu\text{mol}$  SM(PEG)<sub>8</sub> (Thermo Scientific), 20  $\mu\text{mol}$  GGRGDS and 5  $\mu\text{mol}$  Tris(2-carboxyethyl)phosphine (TCEP) in 500 mM  $\text{KH}_2\text{PO}_4$ , pH 7.1, for 18 h at 25  $^{\circ}\text{C}$ . The reaction was purified by ethanol precipitation and then by a NAP-5 column. Purity was analyzed by liquid chromatography–mass spectrometry (LC/MS). If the relative coupling yield was below approximately 50%, the peptide conjugation reaction was repeated. Peptide-DNA conjugates were purified by denaturing gel electrophoresis on a 10% TBE-urea gel (Bio-Rad) at 55  $^{\circ}\text{C}$ . The desired peptide-linked product was recovered by incubating the desired gel slices overnight in 300 mM NaCl twice. Extracted peptide-DNA conjugates were filtered to remove gel fragments and ethanol precipitated. B fragments were 5' phosphorylated by incubating 200 nmol oligonucleotide with 100 U T4 PNK (NEB) in 1 $\times$  CutSmart buffer (NEB) and 400 nmol ATP for 2 h at 37  $^{\circ}\text{C}$ , followed by inactivation of the enzyme for 20 min at 65  $^{\circ}\text{C}$ . The completeness of the phosphorylation reaction was analyzed by LC/MS.

Labeled fragments A and B were ligated by mixing 50 nmol and 70 nmol, respectively, in 1 $\times$  CutSmart Buffer with 100 nmol ATP. For the unstructured (US) control sequence, another 100 nmol DNA splint was added to anneal and ligate the two fragments together. The mixture was heated to 94  $^{\circ}\text{C}$  for 5 min followed by incubation at 25  $^{\circ}\text{C}$  for 15 min. After the fragments were melted and annealed, 8,000 U T4 DNA ligase (NEB) were added, and the mixture was incubated for 16 h at 25  $^{\circ}\text{C}$ . Subsequently, the reaction mixture was ethanol precipitated, dissolved in 80% formamide, and purified by denaturing gel electrophoresis on a 10% TBE/urea gel (Criterion, Bio-Rad) at 65  $^{\circ}\text{C}$ . The desired bands were cut from the gel, and the DNA was extracted twice by addition of 300 mM NaCl, which was followed by filtration, to remove gel debris, and ethanol precipitation. The purity of the product was analyzed by LC/MS. If necessary, gel purification was repeated. Cleavage of the 3' S-S bond was performed with 100 mM DTT in 50 mM  $\text{Na}_2\text{HPO}_4$ , pH 8, at 25  $^{\circ}\text{C}$  for 30 min and followed by gel filtration using a NAP-5 column (GE Healthcare Life Sciences). A different synthesis scheme was deployed for the fluorescein-labeled unfolded control construct, US-fluorescein. It was synthesized on solid support as a single piece with an amino modifier at the 5' end (5'-amino-modifier 5, Glen Research), followed by fluorescein (6-fluorescein phosphoramidite, Glen Research), the oligonucleotide sequence, the epoch eclipse quencher and the 3'-protected thiol modifier (3' thiol modifier C6 SS CPG). After cleavage and work-up as described above, the peptide was appended by incubation of 50 nmol oligonucleotide with 800 nmol bis-NHS cross-linker (BS(PEG)<sub>9</sub>, Thermo Scientific) in 100 mM  $\text{KH}_2\text{PO}_4$ , pH 7.1, at 25  $^{\circ}\text{C}$  for 30 min, followed by addition of 8  $\mu\text{mol}$  GGRGDS and incubation at 25  $^{\circ}\text{C}$  for 18 h. Work-up and thiol deprotection procedures were performed as described above. The purified force probes were analyzed by LC/MS, quantified by UV spectroscopy and lyophilized.

In total, ten TPs, with opening forces ranging from 8.1 to 19.3 pN (measured at 21  $^{\circ}\text{C}$ ), were synthesized from different combinations of hairpins and fluorophores (**Supplementary Tables 1 and 2**). Thermal melting of the TPs demonstrated unfolding-induced fluorescence (**Supplementary Fig. 1**). Several candidate fluorophore-quencher pairs were investigated, on the basis of their spectral overlap and quenching properties, but only

combinations containing fluorescein, Alexa 546, or Alexa 647 as the fluorophore and Epoch Eclipse as the quencher produced robust, cell-dependent fluorescence signals (**Supplementary Table 3**). Immobilization of TPs on surfaces did not appear to disrupt quenching efficiencies (remaining at 97–99%). Oligonucleotides lacking self-complementarity were used as unfolded controls; by design, these did not produce cell-dependent fluorescence. An overview of the synthesis and the sequences of the individual hairpins are given in **Supplementary Tables 1 and 2** and **Supplementary Figure 1**.

**Synthesis and characterization of force probes in optical tweezers experiments.** The synthesis of TPs used for the determinations of opening force was carried out analogously to the method described above. Fragment A contained a 5' adaptor sequence for annealing with complementary sequences, as described previously<sup>1</sup>, followed by a PEG spacer (spacer phosphoramidite 18), fluorescein (6-fluorescein phosphoramidite, Glen Research) and either nucleotides 1–34 of the hairpin sequence for TP9 or nucleotides 1–19 for TP6. Fragment B contained the remaining nucleotides of the force probe at the 5' end followed by the quencher (Epoch Eclipse quencher phosphoramidite), a PEG spacer (spacer phosphoramidite 18) and a 3' adaptor sequence. HPLC purification, phosphorylation and ligation were performed as described above. Unfolding forces, distances and  $F_{1/2}$  values were measured as described previously<sup>16,18</sup> using dual-beam optical tweezers. For TP9 and TP6, the  $F_{1/2}$  values measured in culture medium (at 21 °C) were  $11.3 \pm 0.6$  and  $8.1 \pm 0.7$  pN, respectively, and the opening distances were  $17.6 \pm 0.4$  and  $8.0 \pm 0.2$  nm (mean  $\pm$  s.e.m.). Because fluorophore conjugation and buffer substitution were not found to significantly affect the folding energetics of TP9 (**Fig. 1c** and **Supplementary Table 4**), the  $F_{1/2}$  value for TP17 was taken to be identical to a previously measured value for an unmodified hairpin with the identical sequence (19.3 pN; ref. 16). Unless otherwise noted, the uncertainties reported here for measured parameters were computed from the statistical s.e.m. added in quadrature to estimates of the systematic errors in the measurements<sup>18</sup>.

**Liquid chromatography–mass spectrometry of force probes.** Oligonucleotides were analyzed by LC/MS using a Waters Aquity UPLC coupled to a Waters Q-TOF Premier instrument. 10 pmol sample was run using a linear gradient from 6 mM triethylammonium bicarbonate to 100% methanol over 5 min on an Aquity UPLC BEH C18 column (1.7  $\mu$ m, 2.1 mm  $\times$  100 mm, Waters) at a constant flow rate of 150  $\mu$ L/min. Electrospray ionization was used with a capillary voltage of 3 kV and a sampling cone voltage of 40 V; the detector was operated in negative-ion mode.

**Melting curves of force probes.** Force probes were assayed at a 100–500 nM concentration in PBS or 0.2 $\times$  PBS, 6 M urea on a CFX-96 real-time system with a C1000 thermal cycler (Bio-Rad). After an initial refolding step for 2 min at 94 °C followed by 5 min at 25 °C, the probes were gradually heated to 94 °C while the fluorescence was observed using the predefined settings for FAM (fluorescein-labeled force probes), HEX (Alexa 546–, Cy3– and TAMRA–labeled force probes) and Cy5 (Alexa 647–labeled force probes).

**Functionalization of glass coverslips with TPs.** TPs were covalently attached to glass surfaces through an aminosilane reagent

coupled to a succinimide-PEG-maleimide cross-linker that was reacted with the 3' end of the hairpins<sup>29</sup> (**Supplementary Fig. 1**). Initial studies with multifunctional silanes led to high background signals, prompting us to use a monofunctional ethoxysilane to conjugate only one layer of hairpins to the surface and avoid intramolecular effects or adsorption. Circular coverslips (25-mm diameter, #1 thickness) were sonicated in methanol for 5 min and dried in an oven. They were then plasma cleaned for 5 min (Plasma Prep II, SPI Supplies). 3-(Ethoxydimethylsilyl)propylamine (Sigma) was incubated with the coverslips for functionalization at 3% (v/v) concentration in 200-proof ethanol along with 10% acetic acid aqueous solution as a catalyst at 3% (v/v) concentration (Sigma) for 3 h. The coverslips were then rinsed thoroughly with 200-proof ethanol, dried with nitrogen gas and baked at 110 °C for 1 h. Functionalized coverslips were stored under argon. Upon further functionalization, the coverslips were submerged in borate buffer (BB, 50 mM sodium borate, pH 8.5) for 1 h to protonate the amino group on the silane. A heterobifunctional poly(ethylene glycol) (PEG), which has an amine reactive *N*-hydroxysuccinimide ester (NHS) on one end and a thiol reactive maleimide group on the other, was dissolved in anhydrous dimethylsulfoxide (DMSO) under argon at 250 mM concentration and stored at –20 °C, as per the manufacturer's instruction (Thermo Scientific) (this cross-linker is henceforth referred to as SM(PEG)<sub>2</sub>). SM(PEG)<sub>2</sub> is very sensitive to hydrolysis, so it was divided into aliquots and frozen for one-time use. The SM(PEG)<sub>2</sub> stock was diluted tenfold in BB immediately before use, and the silane-functionalized coverslips were dried with nitrogen gas and incubated in SM(PEG)<sub>2</sub> reaction-buffer for 90 min, then rinsed 4 $\times$  in sterile DI water. TPs were dissolved in a 100  $\mu$ M stock concentration in 10 mM Tris-HCl, pH 7.85, buffer (TB) (Quality Biologicals) with 1 mM MgCl<sub>2</sub> and (Sigma) 1 mM ethylenediaminetetraacetate (EDTA) disodium dihydrate (Gibco) and stored at –20 °C. Prior to conjugation, the TPs were thawed and diluted to 1  $\mu$ M in the same buffer and heated at 90 °C for 5 min and then cooled to room temperature for 10 min to ensure proper folding. TCEP was added to the DNA at a concentration of 10 mM and incubated for 30 min to reduce the thiol at the 3' end. The hairpin solution was then transferred to Amicon Filter 0.5 mL Units (Millipore) with a 3-kDa cutoff and spun in a centrifuge at 16,000g for 30 min to remove TCEP and most of the TB. The tubes were then filled with a coupling buffer (CB), a pH 7.2, 0.1 M sodium phosphate buffer (144.1 mM Na<sub>2</sub>HPO<sub>4</sub>·7H<sub>2</sub>O and 7.25 mM NaH<sub>2</sub>PO<sub>4</sub>·H<sub>2</sub>O). The tubes were then centrifuged again at 16,000g for 30 min to replace the TB with CB. The final volume of the tube was adjusted to match the desired TP concentration during the coupling. 3  $\mu$ M TP concentration during coupling resulted in maximal cell attachment and spreading, with lower surface concentrations resulting in diminished attachment. Coverslips conjugated with SM(PEG)<sub>2</sub> were inserted into Attofluor cell chambers (Invitrogen) for cell seeding and imaging. TPs in CB solution were then added to the coverslips to incubate for 2 h. After the coupling reaction, the coverslips were rinsed with 0.05% Tween 20 to rid the surface of noncovalently attached DNA and then rinsed 4 $\times$  with phosphate buffered saline (PBS). Substrates could be stored overnight at 4 °C in TB and were sufficiently stable to allow cell attachment and study for at least 12 h. However, the substrates are nuclease sensitive, as addition of DNase (DN25, DNase I from bovine

pancreas, 10 mg/mL, Sigma) during imaging of cells attached on TP-conjugated surfaces led to loss of signal and cell detachment within 10 min. To functionalize surfaces with TPs of two different unfolding forces, we conjugated an equimolar mixture of the TPs in CB to activated coverslips, as described above (1.5  $\mu\text{M}$  each to keep the total TP concentration constant at 3  $\mu\text{M}$ ). To vary the amount of TPs bound to surfaces, we coupled different molar ratios of TPs and a 'null' TP (without adhesive peptide and dye) with a fixed total concentration of 3  $\mu\text{M}$ . Changes in background signal of quenched (folded) TPs at different coating densities were negligible, and background subtraction algorithms therefore did not affect estimated measurements of force.

**Imaging and image processing.** TP and cell images were acquired by total-internal-reflection fluorescence (TIRF) microscopy, using a Nikon Eclipse Ti base (Nikon Instruments), an Evolve EMCCD camera (Photometrics) and either a CFI Apo TIRF 60 $\times$  oil (1.49 numerical aperture (NA)) objective or a CFI Plan Fluor 40 $\times$  oil (1.30 NA) objective (Nikon). Live-cell imaging was performed at 37  $^{\circ}\text{C}$  and 5%  $\text{CO}_2$ . TP-functionalized coverslips were inserted into Attofluor cell chambers (Invitrogen). Spontaneously immortalized mouse embryonic fibroblasts (MEFs) (R. Assoian, University of Pennsylvania) or NIH 3T3 cells were trypsinized before imaging and resuspended in a defined medium that contained 0.5 mg cell culture-grade BSA (Invitrogen), 10  $\mu\text{g}/\text{mL}$  insulin (Gibco), 50 ng/mL basic fibroblastic growth factor (bFGF) (Invitrogen), 2  $\mu\text{M}$  hydrocortisone (Sigma), 10  $\mu\text{g}/\text{mL}$  LPA (Sigma), 1% (v/v) penicillin-streptomycin, 1% (v/v) L-glutamine, and a phenol red-free, low-glucose DMEM with no riboflavin (Gibco). Fluorescence images were background subtracted, filtered by a Wiener filter to remove shot noise and band-pass filtered with pass limits reflecting typical sizes for adhesions. The Wiener algorithm calculates the mean,  $\mu$ , and variance,  $\sigma^2$ , around a pixel

$$\mu = \frac{1}{NM} \sum_{n_1, n_2 \in \eta} a(n_1, n_2)$$

and

$$\sigma^2 = \frac{1}{NM} \sum_{n_1, n_2 \in \eta} a^2(n_1, n_2) - \mu^2$$

where  $\eta$  is the  $N \times M$  neighborhood around pixel  $a$ . The filter is then applied to the pixel using the estimate

$$b(n_1, n_2) = \mu + \frac{\sigma^2 - v^2}{\sigma^2} (a(n_1, n_2) - \mu^2)$$

where  $v$  is the noise variance. In these studies the size of the neighborhood was  $3 \times 3$  pixels. Using a Matlab script, we thresholded the images and obtained quantitative metrics of adhesions. An algorithm for tracking the trajectories of geometric centroids of adhesions was used to follow adhesions as they formed or disassembled. The outline of the cell was obtained either by thresholding images of fluorescence-labeled cells or by manually outlining bright-field images. During cytoskeletal tension agonist or antagonist experiments, cells were allowed to spread for 2 h before imaging. At the start of imaging, either 10 mM of Y-27632

or 10  $\mu\text{g}/\text{mL}$  of LPA dissolved in defined medium was added to the live-cell imaging chamber.

**Calibration of TP surface density and pixel intensity to force per unit area.** To calibrate fluorescence intensity with moles of fluorophore at the glass surface, we saturated a glass coverslip functionalized with a silane fluoroalkane (trichloro(1H,1H,2H,2H-perfluorooctyl)silane) by adsorbing 50 mg/mL fluorescently labeled BSA for 1 h, which results in predictable levels of protein and fluorophore on the surface<sup>30</sup>. Imaging conditions identical to those used for TP imaging were then used on these surfaces to calibrate signal intensities to unquenched fluorophores (the number of unfolded TPs) per pixel. Similarly, density of TPs per surface area was determined using a scrambled, unstructured DNA sequence and calibrating against the signal obtained from fluorescent BSA. Coating at 3  $\mu\text{M}$  results in  $\sim 2,700$  TPs per  $\mu\text{m}^2$ . The total force within each pixel required to open this number of TPs then was estimated by multiplying the number of unfolded TPs by its  $F_{1/2}$  value. Because forces higher than the  $F_{1/2}$  value will not further increase signal in a hairpin, the measured signal likely estimates a minimum force being applied. However, the calibration data (**Supplementary Fig. 6**) showing a linear relationship between force and signal for cells on a surface would suggest that the TP population is not saturated under these conditions, and a more complex relationship may exist.

**Application of TPs to other settings.** To test the ability of TPs to report cellular traction forces on substrates other than smooth glass, and cell types beyond MEFs, we conjugated TPs to poly(dimethylsiloxane) (PDMS) surfaces with raised, 1- $\mu\text{m}$ -wide ridges, which induce cells to align along their principal direction. PDMS templates containing raised 1- $\mu\text{m}$ -wide by 1- $\mu\text{m}$ -high troughs were cast from a photoresist-patterned silicon wafer, as previously described<sup>6</sup>. These templates were used to cast inverse features of raised ridges in a thin layer of PDMS on glass coverslips. Substrates were then plasma cleaned in a manner similar to the glass (described above) for 2 min before stamping with 3-(ethoxydimethylsilyl)propylamine (Sigma) followed by rinsing sequentially in 200-proof ethanol, 190-proof ethanol and PBS. Conjugation of the TPs proceeded in an identical fashion as for glass coverslips. Because TIRF was not possible on these substrates, imaging was performed using epifluorescence. TPs revealed polarized localization of traction forces of 3T3 fibroblasts aligned and elongated along the ridge axis, illustrating the potential for assessing forces across multiple types of culture substrates (**Supplementary Fig. 10**).

**Cell culture and transfection.** NIH 3T3 cells (American Type Culture Collection; ATCC, mycoplasma tested) and MEFs (R. Assoian, University of Pennsylvania, mycoplasma tested) were maintained in low-glucose DMEM with 5% FBS and 1% (v/v) penicillin-streptomycin (Invitrogen). Vinculin-mRFP or paxillin-mRFP were expressed in MEFs via transient transfection with Lipofectamine (Invitrogen) or TransIT-LT1 (Mirus) according to the manufacturer's instructions.

**Statistics and analysis.** Statistical tests were conducted as reported in the relevant figure legends. Nonparametric tests were used as indicated for non-normally distributed data sets. Matlab codes

were used to perform the background removal and noise filtering as described in “Imaging and image processing,” as well as analysis of TP signals to report stress per pixel, force per focal adhesion and force per cell as described in the “Calibration” section. Three or more biological replicates were used for all studies, with indicated numbers of cells and adhesions analyzed in each legend

for relevant studies. Cells that did not attach and spread were a minority and were not included in the analyses.

29. Zimmermann, J.L., Nicolaus, T., Neuert, G. & Blank, K. *Nat. Protoc.* **5**, 975–985 (2010).
30. Sigal, G.B., Mrksich, M. & Whitesides, G.M. *J. Am. Chem. Soc.* **120**, 3464–3473 (1998).